Published in final edited form as:
J Comp Neurol. 2006 February 1; 494(4): 635–650. doi:10.1002/cne.20832.

Pyramidal Cells of the Rat Basolateral Amygdala:

Synaptology and Innervation by Parvalbumin-immunoreactive Interneurons

Jay F. Muller, **Franco Mascagni**, and **Alexander J. McDonald***
Department of Pharmacology, Physiology and Neuroscience University of South Carolina School of Medicine Columbia, SC 29208

Abstract

The generation of emotional responses by the basolateral amygdala is largely determined by the balance of excitatory and inhibitory inputs to its principal neurons, the pyramidal cells. The activity of these neurons is tightly controlled by GABAergic interneurons, especially a parvalbumin-positive (PV+) subpopulation that constitutes almost half of all interneurons in the basolateral amygdala. In the present semi-quantitative investigation we studied the incidence of synaptic inputs of PV+ axon terminals onto pyramidal neurons in the rat basolateral nucleus (BLa). Pyramidal cells were identified using calcium/calmodulin-dependent protein kinase II (CaMK) immunoreactivity as a marker. In order to appreciate the relative abundance of PV+ inputs compared to excitatory inputs and other non-PV+ inhibitory inputs, we also analyzed the proportions of asymmetrical (presumed excitatory) synapses and symmetrical (presumed inhibitory) synapses formed by unlabeled axon terminals targeting pyramidal neurons. The results indicate that the perisomatic region of pyramidal cells is innervated almost entirely by symmetrical synapses, whereas the density of asymmetrical synapses increases as one proceeds from thicker proximal dendritic shafts to thinner distal dendritic shafts. The great majority of synapses with dendritic spines are asymmetrical. PV+ axon terminals mainly form symmetrical synapses. These PV+ synapses constitute slightly more than half of the symmetrical synapses formed with each postsynaptic compartment of BLa pyramidal cells. These data indicate that the synaptology of basolateral amygdalar pyramidal cells is remarkably similar to that of cortical pyramidal cells, and that PV+ interneurons provide a robust inhibition of both the perisomatic and distal dendritic domains of these principal neurons.

Keywords

immunocytochemistry; electron microscopy; inhibition, calcium/calmodulin-protein kinase II

The basolateral amygdala (ABL), which consists of the lateral, basolateral, and basomedial amygdalar nuclei, is one of the most important brain regions for the generation of emotional behavior and the formation of emotional memories (Aggleton, 1992; Aggleton, 2000; Shinnick-Gallagher et al., 2003). It receives sensory information from the thalamus and cerebral cortex (McDonald, 1998) and produces appropriate emotional responses by activating a variety of subcortical regions including the central amygdalar nucleus, bed nucleus of the stria terminalis, and striatum. The outputs of the ABL arise from pyramidal cells (McDonald, 1992b), which resemble their counterparts in the cerebral cortex. These neurons, which constitute about 85% of the neurons in the ABL, are characterized by a pyramidal or piriform cell body, and spiny dendrites (Hall, 1972; McDonald, 1982, 1984;

Associate Editor: Joseph L. Price
***Correspondence to:** Alexander J. McDonald Department of Pharmacology, Physiology and Neuroscience University of South Carolina School of Medicine Columbia, SC 29208 Telephone: 803-733-3378 Fax: 803-733-1523 Email: mcdonald@med.sc.edu

1992a,b; Millhouse and DeOlmos, 1983). Some ABL pyramidal cells have a marked pyramidal morphology, with a clear differentiation of thicker “apical” dendrites from thinner “basal” dendrites, whereas others have a semipyramidal or even stellate appearance (McDonald, 1982; 1992). Unlike cortical pyramidal cells, ABL pyramidal cells do not exhibit a laminar organization, and their apical dendrites are not oriented in a parallel manner. Like the cortex, however, ABL pyramidal cells utilize glutamate as an excitatory neurotransmitter (Fuller et al., 1987; McDonald, 1996a; Smith and Paré, 1994).

The generation of emotional responses by the ABL is largely determined by the balance of excitatory and inhibitory inputs to its pyramidal cells (Davis et al., 1994). The cortex and thalamus, as well as neighboring ABL pyramidal neurons, provide excitatory inputs that mainly target dendritic spines of ABL pyramidal cells (Hall, 1972; Carlsen and Heimer, 1988; LeDoux et al., 1991; Stefanacci et al., 1992; Smith and Paré, 1994; Brinley-Reed et al., 1995; Paré et al., 1995; Farb et al., 1999; Smith et al., 2000). Most of the inhibitory inputs, which *in toto* target all postsynaptic domains of ABL pyramidal cells (Carlsen, 1988; McDonald et al., 2002), arise from local GABAergic interneurons. As in the cerebral cortex, these interneurons are spine-sparse nonpyramidal cells that contain calcium-binding proteins (parvalbumin, calbindin, and calretinin) and/or neuropeptides (e.g., vasoactive intestinal peptide, somatostatin, and cholecystokinin) (McDonald and Pearson, 1989; McDonald and Mascagni, 2001; Kemppainen and Pitkänen, 2001). The results of recent double-labeling studies suggest that the ABL contains at least four distinct subpopulations of interneurons that can be distinguished on the basis of their content of calcium-binding proteins and peptides: 1) parvalbumin+/calbindin+ neurons, 2) somatostatin+/calbindin+ neurons, 3) large multipolar cholecystokinin+ neurons that are often calbindin+, and 4) small bipolar and bitufted interneurons that exhibit extensive colocalization of vasoactive intestinal peptide, calretinin, and cholecystokinin (McDonald and Betette, 2001; McDonald and Mascagni, 2001, 2002, Mascagni and McDonald, 2003; Kemppainen and Pitkänen, 2001). Similar interneuronal subpopulations have been identified in the cortex, where it has been shown that each subtype preferentially targets distinct pyramidal cell domains, or other interneurons (Kubota et al., 1994; Kubota and Kawaguchi, 1997; Gonchar and Burkhalter, 1997; Freund and Buzsaki, 1996; Freund, 2003).

ABL interneurons expressing the calcium-binding protein parvalbumin (PV) constitute almost half of all GABAergic interneurons in the rat ABL (McDonald and Mascagni, 2001). Light microscopic studies have demonstrated that axons of PV+ neurons in the ABL form pericellular baskets around the cell bodies of presumed pyramidal neurons, suggesting that some of these cells are basket cells. These baskets are sometimes continuous with PV+ axonal cartridges presumed to represent the axo-axonic contacts of chandelier cells with pyramidal cell axon initial segments. Electron microscopic studies found additional contacts of PV+ axon terminals with dendritic shafts and spines, but it was unclear to what extent these structures belonged to pyramidal neurons versus PV-negative interneurons (Smith et al., 1998). Recent studies in our laboratory have demonstrated that calcium/calmodulin-dependent protein kinase II (CaMK) is a useful marker for pyramidal neurons in ultrastructural studies of ABL synaptology. CaMK is found in the cell bodies and dendrites of all ABL pyramidal neurons, but is not found in GABAergic interneurons (McDonald et al., 2002). In the present investigation we studied the synaptic inputs of PV+ axon terminals onto CaMK+ pyramidal neurons in the rat basolateral nucleus. In order to appreciate the relative abundance of these inputs compared to excitatory inputs and other non-PV+ inhibitory inputs, we also analyzed the proportions of asymmetrical (presumed excitatory) synapses and symmetrical (presumed inhibitory) synapses formed by unlabeled axon terminals targeting pyramidal neurons.

MATERIALS AND METHODS

Tissue preparation and immunocytochemistry

Dual immunocytochemical localization of PV and CaMK, for ultrastructural analysis, was performed in 7 adult male Sprague-Dawley rats (250-350 g; Harlan). Experiments were carried out in accordance with the National Institutes of Health Guide for the Care and Use of Laboratory Animals and were approved by the University of South Carolina Institutional Animal Care and Use Committee. Rats were anesthetized with chloral hydrate (350 mg/kg) and perfused intracardially with 0.1M phosphate buffered saline (PBS; pH 7.4) containing 1% sodium nitrite (50 ml) followed by 4.0% paraformaldehyde-0.2% glutaraldehyde in 0.1 M phosphate buffer (PB; pH 7.4). Brains were then postfixed for 6 hr at 4°C in the fixative used for perfusion. The amygdalar region in each hemisphere was sectioned individually on a vibratome at a thickness of 75 μm in the coronal plane. Selected sections through the anterior subdivision of the basolateral nucleus (BLa) at bregma levels -2.1 through -3.0 (Paxinos and Watson, 1986) were processed for immunohistochemistry in wells of tissue culture plates.

Two protocols for dual localization of PV and CaMK were used: 1) DAB/ immunoperoxidase combined with pre-embedding immunogold-silver (IGS) (n = 4), and 2) a dual immunoperoxidase procedure using DAB and Vector VIP as chromogens (n = 3). For the DAB/IGS technique, sections were incubated in a cocktail of rabbit anti-PV (1:2000; donated by Dr. Kenneth Baimbridge, University of British Columbia) and mouse anti-CaMK (20 μg/ml; Boehringer-Mannheim). Antibodies were diluted in PBS containing 1% normal goat serum (NGS) with 0.03% Triton X-100 and sections were incubated overnight at 4°C. Sections were then processed for the combined immunoperoxidase and preembedding immunogold-silver (IGS) technique (Chan and Pickel, 1990; McDonald et al., 2002). The immunoperoxidase technique, performed first, was used to localize PV, using a Standard Vectastain anti-rabbit ABC kit (Vector Laboratories, Burlingame, CA) with 3,3′-diaminobenzidine (DAB; Sigma, St Louis, MO) as the chromogen. After incubation in a blocking solution, sections were incubated in gold conjugated goat anti-mouse IgG secondary antibody (1:50; AuroProbe One; Amersham, Arlington Height, IL) for 4 hours. Silver intensification was then performed using an Intense-M kit (Amersham) for 7 minutes (McDonald et al., 2002).

For the dual immunoperoxidase procedure using DAB and Vector VIP as chromogens, sections were processed for PV and CaMK immunoreactivity sequentially. Sections were cryoprotected with 30% sucrose in PB, followed by two cycles of freeze-thaw over liquid nitrogen, and rinsed well in PB prior to incubation in rabbit anti-PV (1:3000) in PBS containing 1% NGS overnight at 4°C. Immunoreactivity for PV was then visualized using the DAB technique with the rabbit Elite Vectastain ABC kit (Vector Laboratories, Burlingame, CA) and DAB, followed by a 30 min blocking step using the Vector Avidin-Biotin blocking kit. Sections were then incubated in mouse anti-CaMK (20 μg/ml) in PBS containing 1% NGS overnight at 4°C. After processing the sections with biotinylated goat anti-mouse IgG (1:500; Jackson ImmunoResearch Laboratories, West Grove, PA) and the Elite Vectastain ABC kit (Vector Laboratories, Burlingame, CA), CaMK immunoreactivity was visualized using the Vector VIP (V-VIP) (Vector Laboratories, Burlingame, CA) substrate kit for peroxidase. This procedure yields a reaction product that appears pink/ purple in the light microscope and particulate in the electron microscope (Smiley et al., 1997; Van Haeften and Wouterlood, 2000). The V-VIP reaction was done according to the kit's instructions, but the steps in the subsequent dehydration series were shortened by about 30% to minimize extraction of the pink/purple reaction product (Lanciego, et al., 1997).

After rinsing in buffer, sections were postfixed in osmium tetroxide for 45 minutes: 1% osmium tetroxide in 0.1M PB (pH 7.4) in the first procedure (DAB/IGS), and 2% osmium tetroxide in 0.16 M sodium cacodylate buffer (pH 7.4) in the second procedure (DAB/V-VIP). Sections were dehydrated in a graded ethanol series and acetone, and flat embedded in Polybed 812 (Polysciences) at 60°C. Selected areas of the BLa were remounted onto resin blanks and thin-sectioned at 60-80 nm. Serial sections were collected on formvar coated slot grids, stained with uranyl acetate and Luft's lead citrate, and examined with a JEOL-200CX electron microscope. For quantification (see below), photographic negatives were printed and micrographs were assembled into composites. For publication, negatives were scanned and digitized with a UMAX Power Look III flatbed scanner. Figures were then assembled, labeled, and their components' tonal ranges were adjusted and matched using Photoshop 6.0.

Specificity of the antisera

The CaMK antibody used in this study (#MAB8699, Chemicon International, Temecula CA) is a mouse monoclonal (clone 6G9) which recognizes the alpha subunit of CaMK. The immunogen was purified type II CaMK. The specificity of this antibody, which recognizes both phosphorylated and nonphosphorylated forms of the kinase, has been well-documented in previous studies (Erondu and Kennedy, 1985).

The polyclonal PV antiserum (antiserum R-301; donated by Dr. Kenneth Baimbridge, University of British Columbia), was raised in rabbit and is a widely used antiserum to PV. The immunogen was rat muscle PV. Previous adsorption studies have shown that it recognizes PV, but not other calcium-binding proteins (Conde et al., 1994). Studies conducted in our laboratory have shown that sections incubated in preimmune serum (donated by Dr. Kenneth Baimbridge), normal rabbit serum, or PBS in place of this antibody exhibited no immunostaining (McDonald and Betette, 2001).

Analysis

Semi-quantitative surveys in the two rats with the best ultrastructure and immunocytochemical staining (one processed with the DAB/IGS procedure and one with the DAB/V-VIP procedure) were performed to analyze the distribution of synaptic inputs from PV+ axon terminals and unlabeled axon terminals onto postsynaptic pyramidal cell compartments. In both animals, DAB was used to label PV+ structures. In the electron microscope, DAB-labeled PV+ axon terminals were readily identified by their intense, diffuse, electron-dense reaction product surrounding synaptic vesicles. As previously shown, CaMK immunoreactivity in the rat BLa is exclusively found in pyramidal neurons, although not all distal dendrites and spines are labeled with equal intensity (McDonald et al., 2002). Both the IGS and V-VIP methods used for marking CaMK+ profiles yielded granular reaction products that were easily distinguished from IP-labeled PV+ axon terminals in the electron microscope. Each of these two techniques has advantages and disadvantages. The IGS technique is characterized by the limited penetration of immunogold label, but the silver grains are very distinct. The V-VIP method offers better penetration, similar to DAB, but the granular reaction product varies in electron density. In both preparations, serial section analysis was used extensively to: (1) verify label in small and lightly immunoreactive profiles, (2) identify postsynaptic structures (for example, large-caliber versus small-caliber dendrites, see below), and (3) identify the synaptic nature of appositions involving axon terminals.

In both preparations, areas where both labels were robust were chosen for analysis. In the preparation where CaMK+ pyramidal neurons were labeled with the IGS method, two separate, well-delineated areas were selected. Analysis was confined to the tissue-plastic interface (Chan and Pickel, 1991). In the preparation where the V-VIP method was used for

CaMK localization, one continuous well-delineated area was chosen for analysis. Because of the superior penetration of the V-VIP method, analysis was not confined to the tissue-plastic interface. Within these areas, CaMK+ postsynaptic targets, including perikarya, large-caliber (>1 μm diameter) dendrites, small-caliber (<1 μm diameter) dendrites, spines, and axon initial segments were identified using standard criteria (Peters et al., 1991). Synapses were also identified using standard criteria: parallel presynaptic and postsynaptic membranes separated by a uniform synaptic cleft containing dense intercleft filaments, and clusters of synaptic vesicles associated with the presynaptic membrane. The number of PV-positive and PV-negative axon terminals synapsing with each of these CaMK+ postsynaptic structures was counted. Since pyramidal cell spines are not reliably stained using CaMK antibodies (McDonald et al, 2002), and because the great majority of spines arise from pyramidal cell dendrites (McDonald, 1982; Millhouse and deOlmos, 1983), synaptic inputs to both CaMK-positive and CaMK-negative spines were counted. Synapses were classified as symmetrical or assymmetrical, based on the width of the postsynaptic density (Colonnier, 1968). However, some synapses with spines had postsynaptic densities of intermediate thickness and were designated as “unclassified”. Although many of the axon terminals that formed asymmetrical synapses were CaMK+ (McDonald et al., 2002), the proportions of CaMK+ versus CaMK-negative terminals were not counted.

RESULTS

CaMK and PV immunoreactivity

At the light microscopic level the relationship of PV+ axon terminals to CaMK+ pyramidal cells was most evident when the V-VIP technique was used to visualize CaMK. Many PV+ axon terminals were seen to contact perikarya and proximal dendrites of CaMK+ pyramidal cells, but additional PV+ terminals were seen in the neuropil (Fig. 1). By combining PV and CaMK immunocytochemistry at the electron microscopic level, this study has surveyed the relative proportion and distribution of PV+ terminals, and PV-negative terminals, that innervate the different compartments of pyramidal neurons in the BLa. The two strategies for marking CaMK immunoreactivity (IGS and V-VIP) each had advantages and disadvantages (see Materials and Methods), but ultimately yielded similar results (Table 1).

All PV+ axon terminals forming synapses with perikarya, dendrites and axon initial segments of CaMK+ pyramidal cells formed symmetrical (presumed inhibitory) synapses, consistent with previous studies indicating that PV+ neurons constitute a subpopulation of GABAergic interneurons (Smith et al., 1998, Kemppainen and Pitkänen, 2000; McDonald and Mascagni, 2001). However, a small number of PV+ synapses with spines were associated with thick or intermediate postsynaptic densities, as in the neocortex (Ribak, 1993). Like the neocortex, these PV+ terminals were sometimes observed to form additional synapses with perikarya or dendrites that were symmetrical. To simplify the table, all PV+ synapses with spines have been lumped together, regardless of symmetry (see footnote 2 in Table 1).

Innervation of the perisomatic compartment of CaMK+ pyramidal cells

The perisomatic compartment consists of the soma, axon initial segment, and thick proximal dendrites (>1 μm diameter) of BLa pyramidal cells (see Fig. 5 in McDonald et al., 2002). All synaptic contacts onto CAMK+ perikarya were symmetrical, and about half of these were formed by PV+ axon terminals (Table 1, Figs. 2, 3). The density of synapses, including those formed by PV+ terminals (see also Fig. 1), varied among perikarya, but more extensive sampling and reconstruction will be necessary to determine whether these differences signify distinct populations of pyramidal neurons based on relative densities of

these inputs. Virtually all of the synaptic inputs to some CaMK+ perikarya were from PV+ terminals (Fig. 2).

One CaMK+ axon initial segment was identified in our surveys. It was characterized by fasciculated microtubules and a dense undercoating (Peters et al., 1991). It was partially reconstructed from several serial sections, and a portion is shown in Figure 4. The reconstructed portion was found to receive synaptic contacts from 10 PV+ terminals (Table 1), many of which were arranged in a row (Fig. 4, top six arrows), reminiscent of previously described axonal cartridges of chandelier cells (McDonald, 1982; McDonald and Betette, 2001). This axon initial segment also received symmetrical synaptic contacts from 6 unlabeled terminals, three of which are indicated (Fig. 4, arrowheads).

The great majority (93%) of synapses with shafts of thick (>1 μm diameter) CaMK+ pyramidal cell dendrites were symmetrical and more than half of these symmetrical synapses were formed by PV+ axon terminals (Table 1, Fig. 5).

Innervation of the distal dendritic compartment of CaMK+ pyramidal cells

CaMK+ pyramidal cell dendrites less than 1 μm thick comprise the distal two-thirds of basal dendrites, as well as the distal two-thirds of most branches of apical dendrites (see Fig. 5 in McDonald et al., 2002). The great majority of dendritic spines originate from these dendrites. These spines and their associated thin dendrites comprise the distal dendritic domain of pyramidal cells in the BLa. The great majority (83%) of synapses with shafts of thin (<1 μm diameter) CaMK+ pyramidal cell dendrites were symmetrical and more than half of these symmetrical synapses were formed by PV+ axon terminals (Table 1; Figs. 6-7). PV+ terminals that make synaptic contacts with CaMK+ dendrites often contact other profiles as well, such as neighboring spines (Fig. 6A) or adjacent CaMK+ dendrites (Fig. 6B).

Approximately 20% of the synapses with spines were symmetrical and about half of these were formed by PV+ terminals (Table 1; Figs. 6A, 7-9). A few PV+ terminals forming unclassified or asymmetrical synapses with spines were also seen, but were included in the PV+/symmetrical category for purposes of simplification in the Table (see Footnote 2 in Table 1). Many PV+ axospinous synapses appeared to be formed with the necks or “shoulders” of spines (i.e., at the junction of the spine neck with the dendritic shaft) (Fig. 7). Following spines through serial sections was helpful for locating their dendritic sources (Fig. 8, inset), acquiring more information about the synaptic contacts they receive (Fig. 9), and resolving additional contacts (Fig. 8, inset, Fig. 9). Many spines received inputs from one PV+ terminal forming a symmetrical synapse, and one unlabeled terminal forming an asymmetrical synapse (Figs. 6A, 8, 9). A number of spines were found to receive perforated asymmetrical synapses (Figs. 8, 9, paired arrowheads), some of which were with well-defined CaMK+ spine heads (Fig. 8). Three examples of these perforated synapses are shown to be from CaMK+ terminals (Figs. 8, 9).

DISCUSSION

This is the first investigation to study the proportions of asymmetrical (presumably excitatory) synapses versus symmetrical (presumably inhibitory) synapses in all postsynaptic domains of BLa pyramidal cells. The results indicate that the perisomatic region of pyramidal cells is innervated almost entirely by symmetrical synapses, whereas the density of asymmetrical synapses increases as one proceeds from thicker proximal dendritic shafts to thinner distal dendritic shafts. The great majority of synapses with dendritic spines are asymmetrical. PV+ axon terminals mainly form symmetrical synapses. These PV+ synapses form slightly more than 50% of the symmetrical synapses associated with each

postsynaptic compartment of BLa pyramidal cells. It is of interest in this regard that the PV+ interneuronal subpopulation constitutes about 50% of the GABAergic interneurons in the BLa (McDonald and Mascagni, 2001). In the discussion that follows, the term “basolateral amygdala” (ABL) will be used as a general term to refer to the basolateral nuclear complex as a whole, whereas the term “anterior basolateral nucleus” (BLa) will refer only to that particular nuclear subdivision.

Distribution and relative proportions of symmetrical versus asymmetrical synapses onto pyramidal neurons of the BLa

In light of the many similarities between the cerebral cortex and the ABL, it is of interest that the same distal-to-proximal gradient of asymmetrical versus symmetrical synapses seen in BLa pyramidal cells is also seen in pyramidal cells of the neocortex (Hersch and White, 1981; White and Hersch, 1982; DeFelipe and Farinas, 1992; Alonso-Nanclares et al., 2004). Our findings indicate that 95.6% of asymmetrical (excitatory) synapses are formed with spines, 3.4% with small-caliber CaMK+ dendrites (distal dendrites of pyramidal cells), 1.0% with large-caliber CaMK+ dendrites (proximal dendrites of pyramidal cells), and none with perikarya or axon initial segments of CaMK+ pyramidal cells. These results are consistent with previous electron microscopic studies of ABL inputs. Thus, excitatory glutamatergic inputs from the cerebral cortex (Hall, 1972; Smith and Paré, 1994; Brinley-Reed et al., 1995; Farb et al., 1999; Smith et al., 2000), midline/intralaminar thalamus (Carlsen and Heimer, 1988; LeDoux et al., 1991), and internuclear and intranuclear amygdalar connections (arising from glutamatergic ABL pyramidal neurons; Stefanacci et al., 1992; Smith and Paré, 1994; Paré et al., 1995b; Smith et al., 2000) form asymmetrical synapses with dendritic spines and, to a much lesser extent, thin dendritic shafts in the ABL. Although the great majority of spines arise from dendrites of pyramidal cells (see below), it could not be determined in previous electron microscopic tract-tracing studies to what extent the thin dendritic shafts belonged to pyramidal cells versus interneurons. The finding of axon terminals (including CaMK+ axon terminals) forming asymmetrical synapses with CaMK+ dendritic shafts (McDonald et al., 2002; present study) suggests that some of the thin dendrites belonged to pyramidal cells.

Many spines of BLa pyramidal cells do not exhibit CaMK immunoreactivity (McDonald et al., 2002). However, the results of previous studies suggest that the great majority of spines seen in electron microscopic studies of the BLa belong to pyramidal cells. Golgi studies indicate that pyramidal cell dendrites have a very dense covering of spines, whereas only occasional spines are observed on the dendrites of most nonpyramidal interneurons (McDonald, 1982; Millhouse and deOlmos, 1983). The finding that pyramidal cells constitute 85% of all neurons in the BLa (McDonald, 1992b), and their spine-dense dendritic arborizations are more extensive than those of nonpyramidal cells, suggests that as many as 99% of dendritic spines seen at the electron microscopic level may belong to pyramidal cells. Moreover, although PV+ interneurons (which comprise almost half of all interneurons in the rat BLa) are sparsely-spiny (Muller et al., 2005), their spines were labeled with peroxidase in the present study, and therefore were not included in the analysis of spine synapses (which only analyzed CaMK+ spines and unlabeled spines). However, a moderate density of dendritic spines is obvious on SOM+ neurons in the rat BLa that express NK-1 substance-P-receptor immunoreactivity along their surface plasma membranes (personal observations). Since we have found there are only about 4-5 of these spiny NK-1 immunoreactive cells per 50 μm coronal section through the BLa, compared with several hundred pyramidal cells, the spines of these nonpyramidal cells probably constitute a very small fraction of the unlabeled spines seen in the present study.

Although PV+ axon terminals in the present study always formed symmetrical synapses with somata, axon initial segments, and dendrites, some PV+ synapses with dendritic spines

were asymmetrical. Some of these same terminals also formed symmetrical synapses with adjacent dendrites. Identical results were obtained in the primate hippocampus by Ribak and co-workers (1993). Likewise, in a previous study we observed asymmetrical GABAergic synapses with spines of pyramidal neurons in the rat BLa (McDonald et al., 2002). These data suggest that whereas synaptic symmetry is a useful method for identifying whether most synapses are excitatory or inhibitory, it may not always be useful for determining the functional significance of synapses with dendritic spines. It also suggests that the percentage of inhibitory synapses with spines may be underestimated in studies using only synaptic symmetry to infer whether axospinous synapses are excitatory or inhibitory.

The results of the present study, in conjunction with previous electron microscopic studies (Carlsen, 1988; Aylward and Totterdell, 1993; Smith et al., 2000; McDonald et al., 2002; Muller et al., 2003), indicate that the great majority of symmetrical synapses onto ABL pyramidal cells are formed by several distinct subpopulations of GABAergic interneurons. However, catecholaminergic projections from the brainstem (Asan, 1998) and cholinergic projections from the basal forebrain (Carlsen and Heimer, 1986) may also make a contribution to this population of symmetrical synapses.

Because of the synaptic configuration of BLa pyramidal neurons, excitatory postsynaptic potentials (EPSPs) generated by glutamatergic inputs to dendritic spines and distal dendrites must traverse a gauntlet of inhibitory inputs that target more proximal pyramidal cell domains in order to generate action potentials in the vicinity of the axon initial segment. Likewise, back-propagating action potentials must traverse this same inhibitory gauntlet in the opposite direction to reach distal dendrites and spines.

PV+ inputs to the perisomatic domain of pyramidal neurons

The perisomatic compartment consists of the soma, axon initial segment, and thick proximal dendrites of BLa pyramidal cells. The results of the present study indicate that virtually all of the synapses formed with this compartment are symmetrical, and approximately half are formed by PV+ axon terminals. The robust perisomatic innervation of BLa pyramidal cells by PV+ interneurons was first observed in light microscopic studies in rats (Morys et al., 1999; Kemppainen and Pitkänen, 2000; McDonald and Betette, 2001), monkeys (Pitkänen and Amaral, 1993) and humans (Sorvari et al., 1995), and also in electron microscopic studies in cats (Smith et al., 1998) and humans (Sorvari et al., 1996). Similar results were obtained in the neocortex and hippocampus, where there are actually two separate subpopulations of perisomatic PV+ interneurons: (1) basket cells that have a robust innervation of pyramidal cell somata, and (2) chandelier cells forming “axonal cartridges” that only innervate the axon initial segments of pyramidal cells (Freund and Buzsaki, 1996; Kawaguchi and Kubota, 1998; Maccaferri et al., 2000). Since Golgi studies in the ABL (McDonald and Culberson, 1981; McDonald, 1982) have described chandelier cells whose axons appear to only form axonal cartridges, it appears that the pericellular baskets surrounding ABL pyramidal cell somata may be formed by a separate population of PV+ basket cells.

PV+ chandelier cells in the ABL—There have been very few observations of the innervation of pyramidal cell axon initial segments (AISs) in the ABL at the electron microscopic level. Sorvari and co-workers found numerous “axonal cartridges” formed by PV+ axons enclosing elongated, non-immunostained structures in the human ABL at the light microscopic level (Sorvari et al., 1996). Electron microscopic analysis revealed that these cartridges were formed by PV+ axon terminals forming symmetrical synapses with the AISs of pyramidal cells. Two CaMK+ pyramidal cell AISs that were postsynaptic to numerous GABA+ axon terminals were observed in the rat BLa (McDonald et al., 2002).

Betette and McDonald (1997) described an AIS of a pyramidal cell in the rat BLa that was 30 μm long and was postsynaptic to 17 PV+ axon terminals, and no PV-negative terminals. The CaMK+ AIS of the pyramidal cell seen in the present study was postsynaptic to 16 axon terminals, all forming symmetrical synapses, including 10 intensely-stained PV+ terminals.

ABL chandelier cells were first described in Golgi studies of the opossum amygdala (McDonald and Culberson, 1981), and later in the rat (McDonald, 1982). Since their axons are often myelinated, some of the myelinated PV+ axons seen in the present study may belong to chandelier cells. Axonal collaterals branch to form a local arborization that is 300-400 μm in diameter. Axon terminals on these collaterals are clustered into “axonal cartridges” that are found along a collateral, or on short side branches of the collateral. As in the neocortex and hippocampus (DeFelipe and Farinas, 1992; Soriano et al., 1993) these cartridges vary in length (10-25 μm long) and complexity; some consist simply of a series of 3-8 closely-spaced terminals, whereas others are formed by braid-like collaterals that coil and fold back upon themselves. The latter cartridges typically exhibit 10-15 axon terminals. In Golgi-stained preparations the axon terminals in cartridges have been seen to make intimate synaptic-like contacts with the AISs of ABL pyramidal cells (McDonald and Culberson, 1981; McDonald, 1982).

One Golgi-stained chandelier cell in the rat lateral nucleus, whose axon appeared to be almost entirely confined to the (150-μm-thick) section of origin, formed a total of 126 axonal cartridges within a field that was about 300 um in diameter (see Fig. 14 of McDonald, 1982). Counts of incompletely-visualized axonal arborizations of two chandelier cells in the opossum BLa found 67 and 77 cartridges, respectively (see Figs. 5 and 6 of McDonald and Culberson, 1981). These data suggest that most ABL chandelier cells synapse with the AISs of well over 100 neighboring pyramidal cells. Counts of PV+ axon terminals contacting pyramidal cell AISs in the present study and in previous electron microscopic studies (Sorvari et al., 1996; Betette and McDonald, 1997), as well as counts of PV+ axon terminals in axonal cartridges in material used in a previous light microscopic study in this laboratory (unpublished observations by McDonald and Betette, 2001), suggest that most AISs of ABL pyramidal cells are postsynaptic to 15-30 PV+ axon terminals. These data, in conjunction with the results of Golgi studies (see above) which indicate that individual ABL chandelier cells each contribute about 5-12 axon terminals to each axonal cartridge, suggest that axons from about 2-5 chandelier cells converge on most pyramidal cell AISs in the ABL. These counts are similar to those obtained in the neocortex (DeFelipe and Farinas, 1992) and hippocampus (Buhl et al., 1994).

Although all 17 of the axon terminals forming synapses with the pyramidal cell AIS described by Betette and McDonald (1997) were PV+, only 10 of 16 synapses onto the AIS seen in the present study were PV+. This indicates that other cell types, most likely belonging to other ABL interneuronal subpopulations, also form synapses with pyramidal cell AISs. Likewise, some PV-negative, peptidergic interneurons in the neocortex contribute to the AIS synapses on cortical pyramidal neurons (Lewis and Lund, 1990; Gonchar et al., 2002).

PV+ basket cells in the ABL—Similar to the cortex, the most obvious targets of PV+ neurons in the ABL in light microscopic preparations are the cell bodies and proximal dendrites of pyramidal cells, which are surrounded by pericellular baskets of PV+ axons. These synapses were also seen in electron microscopic studies of the ABL (Sorvari et al., 1996; Smith et al., 1998), where the cell bodies of pyramidal neurons were identified on the basis of their synaptology (i.e., all axo-somatic synapses were symmetrical). In the present study, the identity of these pyramidal cells was confirmed by using CaMK as a pyramidal cell marker. Intracellular labeling studies of individual interneurons in the cortex have

revealed that pericellular baskets surrounding individual pyramidal cells are actually formed by the convergence of axons from many basket cells (Buhl et al., 1994; Miles et al., 1996).

Using light microscopy, we recently analyzed the axonal contacts of several PV+ basket cells in the BLa that were intracellularly labeled with biocytin (A.J. McDonald and D.G. Rainnie, unpublished observations). These cells were seen to form 1-12 contacts with the cell bodies of many neighboring pyramidal cells. The BLa basket cell with the best-stained axon formed an axonal arborization that averaged 600 μm in diameter and made multiple contacts with over 90 Nissl-stained pyramidal cell somata in three 75μm-thick sections. Most pyramidal perikarya received contacts from collaterals forming 4-6 *en passant* contacts. Counts obtained in material used in a previous light microscopic study of PV+ neurons in this laboratory (unpublished observations by McDonald and Betette, 2001), suggest that most cell bodies of BLa pyramidal cells are postsynaptic to 50-80 PV+ axon terminals. These data suggest that roughly 10-20 basket cells may innervate cell bodies of individual BLa pyramidal cells. Similarly, in the hippocampus each basket cell forms 2-5 synapses with each pyramidal cell somata, and it has been estimated that about 25 basket cells innervate cell bodies of individual hippocampal pyramidal cells (Buhl et al., 1994; Miles et al., 1996).

In the present study only about half of the synapses formed with pyramidal cell somata were PV+, indicating that other neuronal populations innervate these perikarya. In the cortex most of these PV-negative synapses are formed by a second population of basket cells containing VIP and/or CCK (Nunzi et al., 1985; Kawaguchi and Kubota, 1996, 1998; Ascady et al, 1996; Maccaferri et al., 2000; Pawelzik et al., 2002). The presence of a significant innervation of BLa pyramidal cell somata by VIP+ axon terminals (Muller et al., 2003) suggests that there may also be a second population of basket cells in this nucleus.

PV+ inputs to the distal dendritic domain of pyramidal neurons

In the present study about half of the synaptic inputs to the shafts of distal dendrites (< 1 μm thick) of CaMK+ pyramidal cells, and 11% of the inputs to dendritic spines, were formed by PV+ axon terminals. It is not clear whether these PV+ inputs come from basket cells or a separate type of PV+ interneuron that selectively targets distal dendrites and spines. Both subpopulations of PV+ cells exist in the cortex. Thus, it is well established that many cortical basket cells, including PV+ basket cells, provide an extensive innervation of distal dendrites and spines in addition to their signature perisomatic innervation of pyramidal cells (Somogyi et al., 1983; Kisvarday et al., 1987; Buhl et al., 1994; Maccaferri et al., 2000). In addition, both the neocortex and hippocampus contain separate subpopulations of PV+ interneurons that selectively target dendritic shafts and spines rather than cell bodies (Pawelzik et al., 2002; Blatow et al., 2003).

In the present study PV+ axon terminals form only about half of the symmetrical synapses with distal dendrites and spines. Most of the remaining symmetrical synapses are probably formed by terminals of the VIP+ and SOM+ GABAergic interneuronal subpopulations (Aylward and Totterdell, 1993; Muller et al., 2003). Our finding that 32.9% of symmetrical synapses were on spines was surprisingly high, but is consistent with a study of the visual cortex that reported a similar percentage (31%; Beaulieu and Colonnier, 1985).

Functional Implications

Since PV+ neurons comprise nearly 50% of GABAergic interneurons in the BLa, their synaptic interactions with pyramidal neurons are extremely important in determining neuronal activity in this region. As mentioned above, excitatory inputs from the cortex and thalamus, which convey specific information related to the emotional and behavioral

significance of sensory stimuli, mainly target the spines and distal dendrites of pyramidal neurons. If the strength of these excitatory inputs is sufficient, these inputs can evoke the firing of the postsynaptic pyramidal cells (e.g., Rainnie et al., 1991). In addition to projections to extrinsic regions, axons of BLa pyramidal cells provide a dense innervation of the dendritic spines of numerous surrounding pyramidal cells (Smith et al., 2000), which could promote synchronous firing of these cells (Paré and Gaudreau, 1996).

Pyramidal cells also provide a robust innervation of the perisomatic domain, and a sparser innervation of the dendritic domain, of many neighboring PV+ interneurons (Morys et al. 1999; Smith et al., 2000; McDonald et al., 2005). This innervation pattern suggests that pyramidal cells provide a robust excitatory drive to PV+ interneurons. Since spontaneous EPSCs in fast-spiking basolateral interneurons (most likely representing PV+ neurons) are of high amplitude (Mahanty and Sah, 1998; Rainnie, 1999), and populations of pyramidal cells in the BLa often fire in synchronous bursts (Paré et al., 1995a; Paré and Gaudreau, 1996), it seems likely that PV+ interneurons could easily reach firing threshold in response to excitation from pyramidal cell discharge, particularly since individual PV+ interneurons are probably innervated by more than one pyramidal cell. As in the cortex (Geiger et al., 1997), excitatory drive onto putative PV+ interneurons in the basolateral nucleus exhibits rapid kinetics that appears to be mediated primarily by GluR1 AMPA receptors (Mahanty and Sah, 1998; McDonald , 1996; Woodruff and Sah, 2003). In response to pyramidal cell excitation, PV+ basket cells and chandelier cells could provide robust perisomatic feedback inhibition of pyramidal cells. This would also be very rapid due to the close proximity of these inputs to the site of axon potential initiation, and because this perisomatic inhibition is mediated by activation of α_1-subunit-containing $GABA_A$ receptors that exhibit fast kinetics (Woodruff and Sah, 2003). The high speed and temporal precision of these reciprocal pyramidal cell-PV interconnections is probably critical for the generation of rhythmic oscillations in the basolateral amygdala (Paré et al., 2002).

During the last decade it has become evident that the functional activity of many brain areas is dependent upon fast synchronous oscillations of large populations of interconnected neurons (Singer, 1993). Synchronous firing of interconnected neuronal assemblies permits temporal coding of information and promotes synaptic plasticity (Singer 1993; Buzsaki, 2002). Several different rhythms have been observed both within and across different cortical areas including theta (4-10 Hz), gamma (30-100 Hz), and ultrafast (ca. 200 Hz) oscillations. It has been shown that a network of PV+ basket cells and chandelier cells in the cortex, interconnected by dendritic gap junctions and GABAergic chemical synapses, plays an important role in the generation and maintenance of these oscillations (Freund and Buzsaki, 1996; Freund, 2003). This network can entrain the firing of neighboring pyramidal cells via a robust, inhibitory, perisomatic innervation.

Recent studies have demonstrated that prominent theta and gamma oscillations occur in the basolateral amygdala during emotional arousal (Paré and Collins, 2000; Paré et al., 2002; Oya et al., 2002; Seidenbecher et al., 2003). We have recently documented that the BLa, like the cortex, contains networks of PV+ neurons interconnected by gap junctions and GABAergic synapses (Muller et al., 2005). As in the cortex (Whittington et al., 1995; Whittington and Traub, 2003; Freund, 2003) these networks of PV+ interneurons in the BLa are probably important for the generation of gamma and theta rhythms. The extensive divergence and convergence of the axons of BLa basket cells and chandelier cells synapsing with the perisomatic domains of numerous surrounding pyramidal cells could entrain the firing of these cells. The myelination of the axons of these interneurons (see above) might help to synchronize the outputs of these PV+ neurons over their entire axonal arborization. Rebound firing of the inhibited pyramidal cells (Washburn and Moises, 1992; Rainnie et al., 1993; Paré et al., 1995) would result in reactivation of the PV+ interneuronal network. This

proposed mechanism would predict that PV+ basket cells and chandelier cells would fire counterphase to pyramidal cells, as in the cortex (Freund and Buzsaki, 1996; Freund, 2003). This is consistent with electrophysiological studies in the basolateral nucleus that have demonstrated counterphase firing of pyramidal cells and interneurons during delta and theta rhythms (Paré and Gaudreau, 1996). There is evidence that these network rhythms, as well as intrinsic oscillations in ABL pyramidal cells (Pape et al., 1998), are critical for synaptic plasticity associated with the formation of emotional memories (Paré et al, 2002; Pape and Stork, 2003).

Acknowledgments

The authors would like to thank Dr. Kenneth Baimbridge, University of British Columbia, for his generous gift of the antibody to parvalbumin.

Grant Sponsor: National Institutes of Health Grant NS38998

LITERATURE CITED

Aggleton, JP. The Amygdala: Neurobiological Aspects of Emotion, Memory, and Mental Dysfunction. Wiley-Liss; New York: 1992.

Aggleton, JP. The Amygdala: A Functional Analysis. Wiley-Liss; New York: 2000.

Alonso-Nanclares L, White EL, Elston GN, DeFelipe J. Synaptology of the proximal segment of pyramidal cell basal dendrites. Eur J Neurosci. 2004; 19:771–6. [PubMed: 14984428]

Asan E. The catecholaminergic innervation of the rat amygdala. Adv Anat Embryol Cell Biol. 1998; 142:1–118. [PubMed: 9586282]

Acsady L, Arabadzisz D, Freund TF. Correlated morphological and neurochemical features identify different subsets of vasoactive intestinal polypeptide-immunoreactive interneurons in rat hippocampus. Neuroscience. 1996; 73:299–315. [PubMed: 8783251]

Aylward RL, Totterdell S. Neurons in the ventral subiculum, amygdala and entorhinal cortex which project to the nucleus accumbens: their input from somatostatin-immunoreactive boutons. J Chem Neuroanat. 1993; 6:31–42. [PubMed: 7679909]

Beaulieu C, Colonnier MA. A laminar analysis of the number of round-asymmetrical and flat-symmetrical synapses on spines, dendritic trunks, and cell bodies in area 17 of the cat. J Comp Neurol. 1985; 231:180–189. [PubMed: 3968234]

Betette RL, McDonald AJ. Differential innervation of basolateral amygdalar neurons by distinct subpopulations of local circuit neurons. Soc Neurosci Abst. 1997; 23:2101.

Blatow M, Rozov A, Katona I, Hormuzdi SG, Meyer AH, Whittington MA, Caputi A, Monyer H. A novel network of multipolar bursting interneurons generates theta frequency oscillations in neocortex. Neuron. 2003; 38:805–817. [PubMed: 12797964]

Brinley-Reed M, Mascagni F, McDonald AJ. Synaptology of prefrontal cortical projections to the basolateral amygdala: an electron microscopic study in the rat. Neurosci Lett. 1995; 202:45–48. [PubMed: 8787827]

Buhl EH, Halasy K, Somogyi P. Diverse sources of hippocampal unitary inhibitory postsynaptic potentials and the number of synaptic release sites. Nature. 1994; 368:823–8. [PubMed: 8159242]

Buzsaki G. Theta oscillations in the hippocampus. Neuron. 2002; 33:325–40. [PubMed: 11832222]

Carlsen J. Immunocytochemical localization of glutamate decarboxylase in the rat basolateral amygdaloid nucleus, with special reference to GABAergic innervation of amygdalostriatal projection neurons. J Comp Neurol. 1988; 273:513–526. [PubMed: 3062049]

Carlsen J, Heimer L. A correlated light and electron microscopic immunocytochemical study of cholinergic terminals and neurons in the rat amygdaloid body with special emphasis on the basolateral amygdaloid nucleus. J Comp Neurol. 1986; 244:121–136. [PubMed: 3512630]

Carlsen J, Heimer L. The basolateral amygdaloid complex as a cortical-like structure. Brain Res. 1988; 441:377–80. [PubMed: 2451985]

Chan J, Aoki C, Pickel VM. Optimization of differential immunogold-silver and peroxidase labeling with maintenance of ultrastructure in brain sections before plastic embedding. J Neurosci Methods. 1990; 33:113–127. [PubMed: 1977960]

Collins DR, Pelletier JG, Paré D. Slow and fast (gamma) neuronal oscillations in the perirhinal cortex and lateral amygdala. J Neurophysiol. 2001; 85:1661–1672. [PubMed: 11287489]

Colonnier M. Synaptic patterns on different cell types in the different laminae of the cat visual cortex. An electron microscope study. Brain Res. 1968; 9:268–87. [PubMed: 4175993]

Conde F, Lund JS, Jacobowitz DM, Baimbridge KG, Lewis DA. Local circuit neurons immunoreactive for calretinin, calbindin D-28k or parvalbumin in monkey prefrontal cortex: distribution and morphology. J Comp Neurol. 1994; 341:95–116. [PubMed: 8006226]

Davis M, Rainnie D, Cassell M. Neurotransmission in the rat amygdala related to fear and anxiety. Trends Neurosci. 1994; 17:208–14. [PubMed: 7520203]

DeFelipe J, Farinas I. The pyramidal neuron of the cerebral cortex: morphological and chemical characteristics of the synaptic inputs. Prog Neurobiol. 1992; 39:563–607. [PubMed: 1410442]

Farb CR, Ledoux JE. Afferents from rat temporal cortex synapse on lateral amygdala neurons that express NMDA and AMPA receptors. Synapse. 1999; 33:218–29. [PubMed: 10420169]

Erondu NE, Kennedy MB. Regional distribution of type II Ca2+/calmodulin-dependent protein kinase in rat brain. J Neurosci. 1985; 5:3270–7. [PubMed: 4078628]

Freund TF. Interneuron Diversity series: Rhythm and mood in perisomatic inhibition. Trends Neurosci. 2003; 26:489–95. [PubMed: 12948660]

Freund TF, Buzsáki G. Interneurons of the hippocampus. Hippocampus. 1996; 6:347–470. [PubMed: 8915675]

Fuller TA, Russchen FT, Price JL. Sources of presumptive glutamergic/aspartergic afferents to the rat ventral striatopallidal region. J Comp Neurol. 1987; 258:317–338. [PubMed: 2884240]

Geiger JR, Lubke J, Roth A, Frotscher M, Jonas P. Submillisecond AMPA receptor-mediated signaling at a principal neuron-interneuron synapse. Neuron. 1997; 18:1009–1023. [PubMed: 9208867]

Gonchar Y, Burkhalter A. Three distinct families of GABAergic neurons in rat visual cortex. Cerebral Cortex. 1997; 7:347–358. [PubMed: 9177765]

Gonchar Y, Turney S, Price JL, Burkhalter A. Axo-axonic synapses formed by somatostatin-expressing GABAergic neurons in rat and monkey visual cortex. J Comp Neurol. 2002; 443:1–14. [PubMed: 11793343]

Hersch SM, White EL. Quantification of synapses formed with apical dendrites of Golgi-impregnated pyramidal cells: variability in thalamocortical inputs, but consistency in the ratios of asymmetrical to symmetrical synapses. Neuroscience. 1981; 6:1043–1051. [PubMed: 7279213]

Hall E. The amygdala of the cat: a Golgi study. Z Zellforsch. 1972; 134:439–458. [PubMed: 4638299]

Kawaguchi Y, Kubota Y. Physiological and morphological identification of somatostatin- or vasoactive intestinal polypeptide-containing cells among GABAergic cell subtypes in rat frontal cortex. J. Neurosci. 1996; 16:2701–2715. [PubMed: 8786446]

Kawaguchi Y, Kubota Y. Neurochemical features and synaptic connections of large physiologically-identified GABAergic cells in the rat frontal cortex. Neuroscience. 1998; 85:677–701. [PubMed: 9639265]

Kemppainen S, Pitkänen A. Distribution of parvalbumin, calretinin, and calbindin-D_{28k} immunoreactivity in the rat amygdaloid complex and colocalization with gamma-aminobutyric acid. J Comp Neurol. 2000; 426:441–467. [PubMed: 10992249]

Kisvarday ZF, Martin KA, Friedlander MJ, Somogyi P. Evidence for interlaminar inhibitory circuits in the striate cortex of the cat. J Comp Neurol. 1987; 260:1–19. [PubMed: 3597830]

Kubota Y, Hattori R, Yui Y. Three distinct subpopulations of GABAergic neurons in rat frontal agranular cortex. Brain Res. 1994; 649:159–173. [PubMed: 7525007]

Kubota Y, Kawaguchi Y. Two distinct subgroups of cholecystokinin-immunoreactive cortical interneurons. Brain Res. 1997; 752:175–183. [PubMed: 9106454]

Lanciego JL, Goede PH, Witter MP, Wouterlood FG. Use of peroxidase substrate Vector VIP for multiple staining in light microscopy. J Neurosci Methods. 1997; 74:1–7. [PubMed: 9210569]

LeDoux JE, Farb CR, Milner TA. Ultrastructure and synaptic associations of auditory thalamo-amygdala projections in the rat. Exp Brain Res. 1991; 85:577–586. [PubMed: 1717305]

Mascagni F, McDonald AJ. Immunohistochemical characterization of cholecystokinin containing neurons in the rat basolateral amygdala. Brain Res. 2003; 976:171–184. [PubMed: 12763251]

McDonald AJ. Neurons of the lateral and basolateral amygdaloid nuclei: a Golgi study in the rat. J Comp Neurol. 1982; 212:293–312. [PubMed: 6185547]

McDonald AJ. Neuronal organization of the lateral and basolateral amygdaloid nuclei in the rat. J Comp Neurol. 1984; 222:589–606. [PubMed: 6199387]

McDonald, AJ. Cell types and intrinsic connections of the amygdala. In: Aggleton, JP., editor. The Amygdala. Wiley-Liss; New York: 1992a. p. 67-96.

McDonald AJ. Projection neurons of the basolateral amygdala: a correlative Golgi and retrograde tract tracing study. Brain Res Bull. 1992b; 28:179–185. [PubMed: 1375860]

McDonald AJ. Glutamate and aspartate immunoreactive neurons of the rat basolateral amygdala: colocalization of excitatory amino acids and projections to the limbic circuit. J Comp Neurol. 1996a; 365:367–379. [PubMed: 8822176]

McDonald AJ. Localization of AMPA glutamate receptor subunits in subpopulations of non-pyramidal neurons in the rat basolateral amygdala. Neurosci Lett. 1996b; 208:175–8. [PubMed: 8733298]

McDonald AJ. Cortical pathways to the mammalian amygdala. Prog Neurobiol. 1998; 55:257–332. [PubMed: 9643556]

McDonald AJ, Culberson JL. Neurons of the basolateral amygdala: a Golgi study in the opossum (Didelphis virginiana). Am J Anat. 1981; 162:327–42. [PubMed: 7325125]

McDonald AJ, Pearson JC. Coexistence of GABA and peptide immunoreactivity in nonpyramidal neurons of the basolateral amygdala. Neurosci Lett. 1989; 100:53–58. [PubMed: 2569703]

McDonald AJ, Betette R. Parvalbumin containing neurons in the rat basolateral amygdala: morphology and colocalization of calbindin D-28k. Neuroscience. 2001; 102:413–425. [PubMed: 11166127]

McDonald AJ, Mascagni F. Colocalization of calcium-binding proteins and GABA in neurons of the rat basolateral amygdala. Neuroscience. 2001; 105:681–693. [PubMed: 11516833]

McDonald AJ, Muller JF, Mascagni F. GABAergic innervation of alpha type II calcium/calmodulin-dependent protein kinase immunoreactive pyramidal neurons in the rat basolateral amygdala. J Comp Neurol. 2002; 446:199–218. [PubMed: 11932937]

McDonald AJ, Mascagni F. Immunohistochemical characterization of somatostatin containing interneurons in the rat basolateral amygdala. Brain Res. 2002; 943:237–244. [PubMed: 12101046]

McDonald AJ, Mascagni F, Mania I, Rainnie DG. Evidence for a perisomatic innervation of parvalbumin-containing interneurons by individual pyramidal cells in the basolateral amygdala. Brain Res. 2005; 1035:32–40. [PubMed: 15713274]

Miles R, Toth K, Gulyas AI, Hajos N, Freund TF. Differences between somatic and dendritic inhibition in the hippocampus. Neuron. 1996; 16:815–823. [PubMed: 8607999]

Millhouse OE, DeOlmos J. Neuronal configurations in lateral and basolateral amygdala. Neuroscience. 1983; 10:1269–1300. [PubMed: 6664494]

Morys J, Berdel B, Kowianski P, Majak K, Tarnawski M, Wisniewski HM. Relationship of calcium-binding protein containing neurons and projection neurons in the rat basolateral amygdala. Neurosci Lett. 1999; 259:91–4. [PubMed: 10025565]

Muller JF, Mascagni F, McDonald AJ. Synaptic connections of distinct interneuronal subpopulations in the rat basolateral amygdalar nucleus. J Comp Neurol. 2003; 456:217–236. [PubMed: 12528187]

Muller JF, Mascagni F, McDonald AJ. Coupled networks of parvalbumin-immunoreactive interneurons in the rat basolateral amygdala. J. Neuroscience. 2005; 25:7366–7376.

Nunzi MG, Gorio A, Milan F, Freund TF, Somogyi P, Smith AD. Cholecystokinin-immunoreactive cells form symmetrical synaptic contacts with pyramidal and nonpyramidal neurons in the hippocampus. J Comp Neurol. 1985; 237:485–505. [PubMed: 4044896]

Oya H, Kawasaki H, Howard MA 3rd, Adolphs R. Electrophysiological responses in the human amygdala discriminate emotion categories of complex visual stimuli. J Neurosci. 2002; 22:9502–9512. [PubMed: 12417674]

Pape HC, Paré D, Driesang RB. Two types of intrinsic oscillations in neurons of the lateral and basolateral nuclei of the amygdala. J Neurophysiol. 1998; 79:205–216. [PubMed: 9425192]

Pape HC, Stork O. Genes and mechanisms in the amygdala involved in the formation of fear memory. Ann N Y Acad Sci. 2003; 985(2003):92–105. [PubMed: 12724151]

Paré D, Pape HC, Dong J. Bursting and oscillating neurons of the cat basolateral amygdaloid complex in vivo: electrophysiological properties and morphological features. J Neurophysiol. 1995a; 74:1179–91.

Paré D, Smith Y, Paré JF. Intra-amygdaloid projections of the basolateral and basomedial nuclei in the cat: Phaseolus vulgaris-leucoagglutinin anterograde tracing at the light and electron microscopic level. Neuroscience. 1995b; 69:567–83.

Paré D, Gaudreau H. Projection cells and interneurons of the lateral and basolateral amygdala: distinct firing patterns and differential relation to theta and delta rhythms in conscious cats. J Neurosci. 1996; 16:3334–3350. [PubMed: 8627370]

Paré D, Collins DR. Neuronal correlates of fear in the lateral amygdala: multiple extracellular recordings in conscious cats. J Neurosci. 2000; 20:2701–2710. [PubMed: 10729351]

Paré D, Collins DR, Pelletier JG. Amygdala oscillations and the consolidation of emotional memories. Trends Cogn Sci. 2002; 6:306–314. [PubMed: 12110364]

Pawelzik H, Hughes DI, Thomson AM. Physiological and morphological diversity of immunocytochemically defined parvalbumin- and cholecystokinin-positive interneurones in CA1 of the adult rat hippocampus. J Comp Neurol. 2002; 443:346–67. [PubMed: 11807843]

Paxinos, G.; Watson, C. Academic Press; New York: 1986. The Rat Brain in Stereotaxic Coordinates.

Peters, A.; Palay, SL.; Webster, HD. The fine structure of the nervous system. Oxford University Press; New York: 1991.

Pitkänen A, Amaral DG. Distribution of parvalbumin-immunoreactive cells and fibers in the monkey temporal lobe: The amygdaloid complex. J Comp Neurol. 1993; 331:14–36. [PubMed: 8320347]

Rainnie DG. Serotonergic modulation of neurotransmission in the rat basolateral amygdala. J. Neurophysiol. 1999; 82:69–85. [PubMed: 10400936]

Rainnie DG, Asprodini EK, Shinnick-Gallagher P. Excitatory transmission in the basolateral amygdala. J Neurophysiol. 1991; 66:986–998. [PubMed: 1684383]

Rainnie DG, Asprodini EK, Shinnick-Gallagher P. Intracellular recordings from morphologically identified neurons of the basolateral amygdala. J Neurophysiol. 1993; 69:1350–1361. [PubMed: 8492168]

Ribak CE, Seress L, Leranth C. Electron microscopic immunocytochemical study of the distribution of parvalbumin-containing neurons and axon terminals in the primate dentate gyrus and Ammon's horn. J Comp Neurol. 1993; 327:298–321. [PubMed: 8425946]

Seidenbecher T, Laxmi TR, Stork O, Pape HC. Amygdalar and hippocampal theta rhythm synchronization during fear memory retrieval. Science. 2003; 301:846–50. [PubMed: 12907806]

Shinnick-Gallagher, P.; Pitkanen, A.; Shekhar, A.; Cahill, L. Ann N Y Acad Sci. Vol. 985. The New York Academy of Sciences; New York: 2003. The Amygdala in Brain Function: Basic and Clinical Approaches.

Singer W. Synchronization of cortical activity and its putative role in information processing and learning. Annu Rev Physiol. 1993; 55:349–374. [PubMed: 8466179]

Smiley JF, Morrell F, Mesulam MM. Cholinergic synapses in human cerebral cortex: an ultrastructural study in serial sections. Exp Neurol. 1997; 144:361–8. [PubMed: 9168836]

Smith Y, Paré D. Intra-amygdaloid projections of the lateral nucleus in the cat: PHA-L anterograde labeling combined with postembedding GABA and glutamate immunocytochemistry. J. Comp. Neurol. 1994; 342:232–248. [PubMed: 7911130]

Smith Y, Paré J-F, Paré D. Cat intraamygdaloid inhibitory network: Ultrastructural organization of parvalbumin-immunoreactive elements. J Comp Neurol. 1998; 391:164–179. [PubMed: 9518267]

Smith Y, Paré J-F, Paré D. Differential innervation of parvalbumin-immunoreactive interneurons of the basolateral amygdaloid complex by cortical and intrinsic inputs. J Comp Neurol. 2000; 416:496–508. [PubMed: 10660880]

Somogyi P, Kisvarday ZF, Martin KA, Whitteridge D. Synaptic connections of morphologically identified and physiologically characterized large basket cells in the striate cortex of cat. Neuroscience. 1983; 10:261–94. [PubMed: 6633861]

Soriano E, Martinez A, Farinas I, Frotscher M. Chandelier cells in the hippocampal formation of the rat: the entorhinal area and subicular complex. J Comp Neurol. 1993; 337:151–67. [PubMed: 8276990]

Sorvari H, Soininen H, Paljärvi L, Karkola K, Pitkänen A. Distribution of parvalbumin immunoreactive cells and fibers in the human amygdaloid complex. J Comp Neurol. 1995; 360:185–212. [PubMed: 8522643]

Sorvari H, Miettinin R, Soininen H, Pitkänen A. Parvalbumin-immunoreactive neurons make inhibitory synapses on pyramidal cells in the human amygdala: a light and electron microscopic study. Neurosci Lett. 1996; 217:93–96. [PubMed: 8916080]

Stefanacci L, Farb CR, Pitkänen A, Go G, LeDoux JE, Amaral DG. Projections from the lateral nucleus to the basal nucleus of the amygdala: a light and electron microscopic PHA-L study in the rat. J Comp Neurol. 1992; 323:586–601. [PubMed: 1430325]

Van Haeften T, Wouterlood FG. Neuroanatomical tracing at high resolution. J Neurosci Methods. 2000; 103:107–116. [PubMed: 11074100]

Washburn MS, Moises HC. Electrophysiological and morphological properties of rat basolateral amygdaloid neurons *in vitro*. J Neurosci. 1992; 12:4066–4079. [PubMed: 1403101]

White EL, Hersch SM. A quantitative study of thalamocortical and other synapses involving the apical dendrites of corticothalamic projection cells in mouse SmI cortex. J Neurocytol. 1982; 11:137–57. [PubMed: 6174701]

Whittington MA, Traub RD, Jefferys JG. Synchronized oscillations in interneuron networks driven by metabotropic glutamate receptor activation. Nature. 1995; 373:612–615. [PubMed: 7854418]

Whittington MA, Traub RD. Interneuron diversity series: inhibitory interneurons and network oscillations in vitro. Trends Neurosci. 2003; 26:676–82. [PubMed: 14624852]

Woodruff, AR.; Sah, P. 2003 Abstract Viewer/Itinerary Planner. Society for Neuroscience; Washington, DC: 2003. Properties of parvalbumin-positive interneurons in the basolateral amygdala.

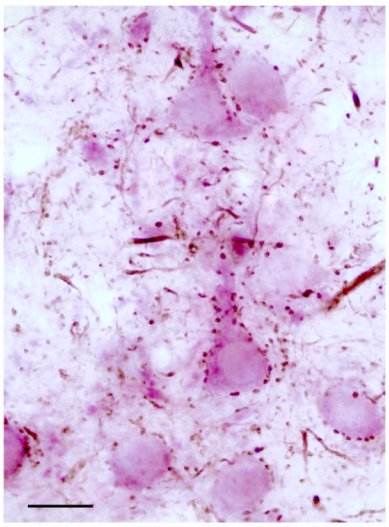

Figure 1.
Light micrograph illustrating the innervation of CaMK+ pyramidal cell perikarya and proximal dendrites labeled by the V-VIP peroxidase technique (purple), by PV+ axon terminals labeled by the DAB peroxidase technique (brown). Scale bar = 20 μm.

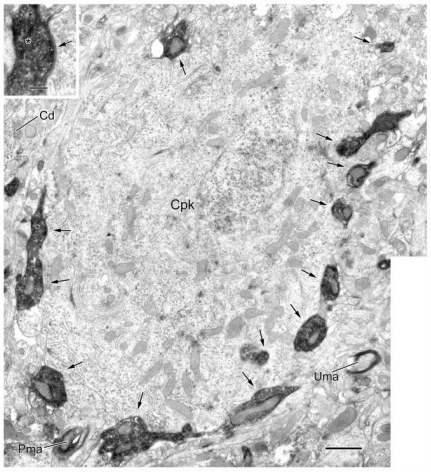

Figure 2.

Electron micrographic composite of a CaMK+ pyramidal cell perikaryon (Cpk) innervated by PV+ axon terminals (arrows). PV+ terminals are clearly marked with intense DAB reaction product; all 13 synapses indicated were confirmed through serial sections. The inset shows a magnified view of one PV+ terminal (asterisk) and its synaptic contact. The moderately dense, particulate V-VIP reaction product for CaMK immunoreactivity is more obvious, at this low magnification, in the neighboring CaMK+ dendrites (Cd) than in the perikaryon (Cpk), where it is somewhat obscured by cytosolic features such as polysomes (see Fig. 3). An oblique view of a PV+ myelinated axon (Pma) is also indicated, with an unlabeled myelinated axon profile (Uma) shown for comparison. Scale bars = 1 μm, 0.2 μm for inset.

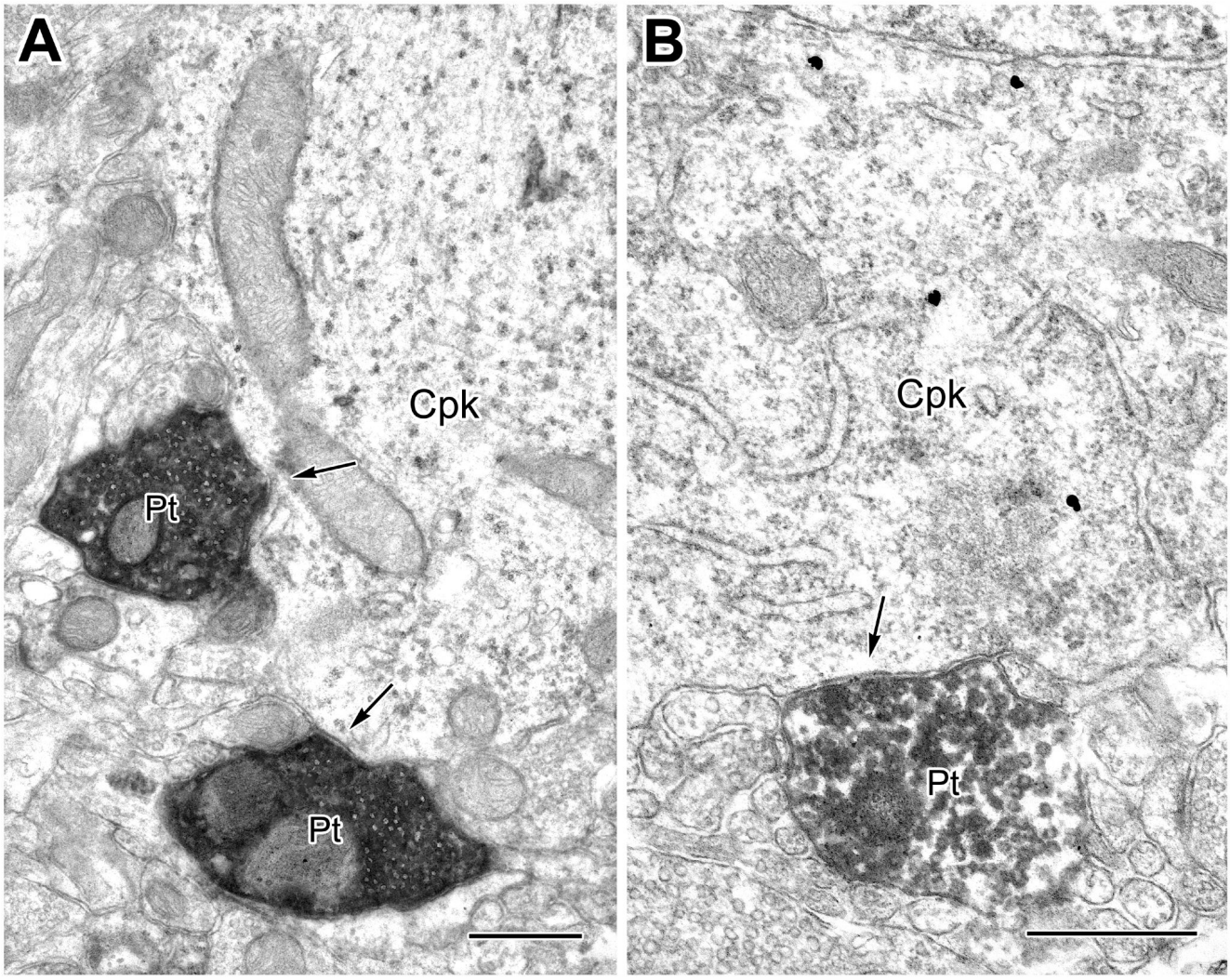

Figure 3.

Electron micrographs of CaMK+ pyramidal cell perikarya receiving synaptic inputs from PV+ terminals (Pt). **A:** A CaMK+ perikaryon (Cpk) receives input (arrows) from two PV+ terminals (Pt). The particulate V-VIP reaction product for CaMK is clearly distinguishable from other perikaryal features at this magnification (compared to Fig. 2). The axosomatic synapse of the upper PV+ terminal was seen more clearly in adjacent serial sections; this terminal also synapses with a thin unlabeled dendrite located below the terminal. **B:** A PV+ terminal (Pt) makes synaptic contact (arrow) onto a CaMK+ perikaryon (Cpk) labeled by the IGS technique, with 4 silver grains apparent in this view. Scale bars = 0.5 μm.

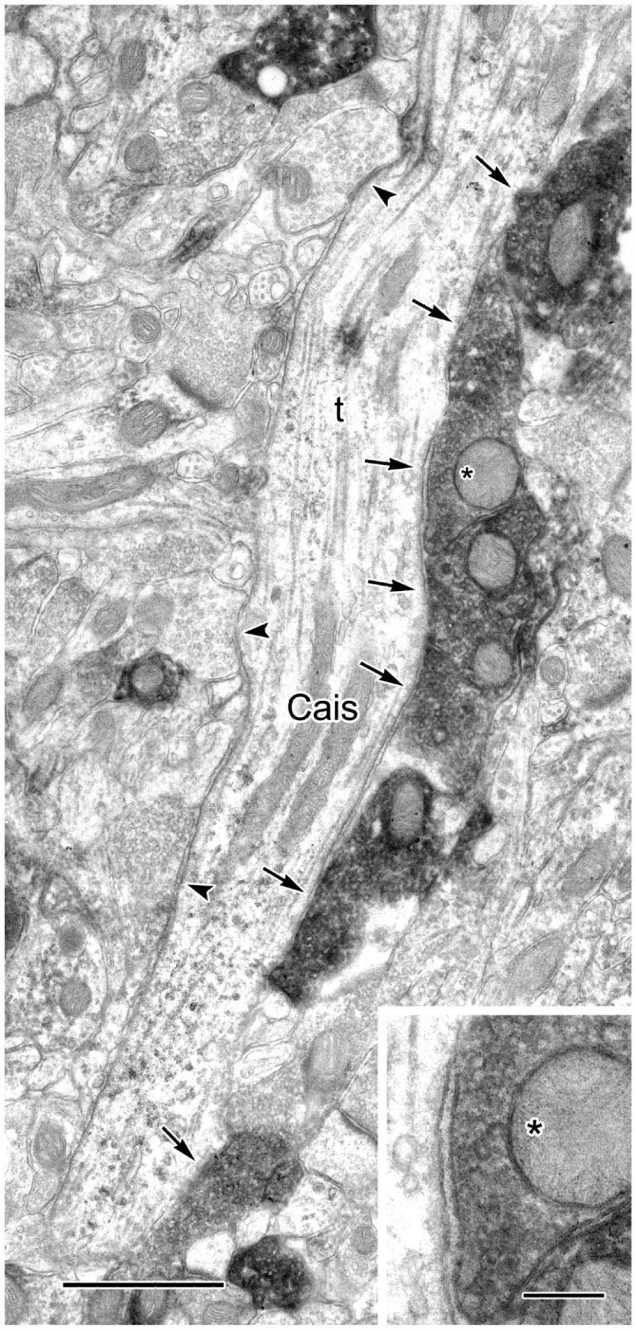

Figure 4.

A CaMK+ axon initial segment (Cais), labeled by the V-VIP method, receives symmetrical synaptic inputs from PV+ axon terminals (arrows) and unlabeled terminals (arrowheads). Five of the PV+ terminals shown are adjacent to one another (top five arrows). One of these PV+ terminals (asterisk) is shown magnified in the inset. This CAMK+ axon initial segment was followed through four additional serial sections (from the upper right of the field shown). The synaptic nature of each of these axoaxonic contacts was ascertained in these serial sections. Scale bars = 1 μm, 0.25 μm for inset.

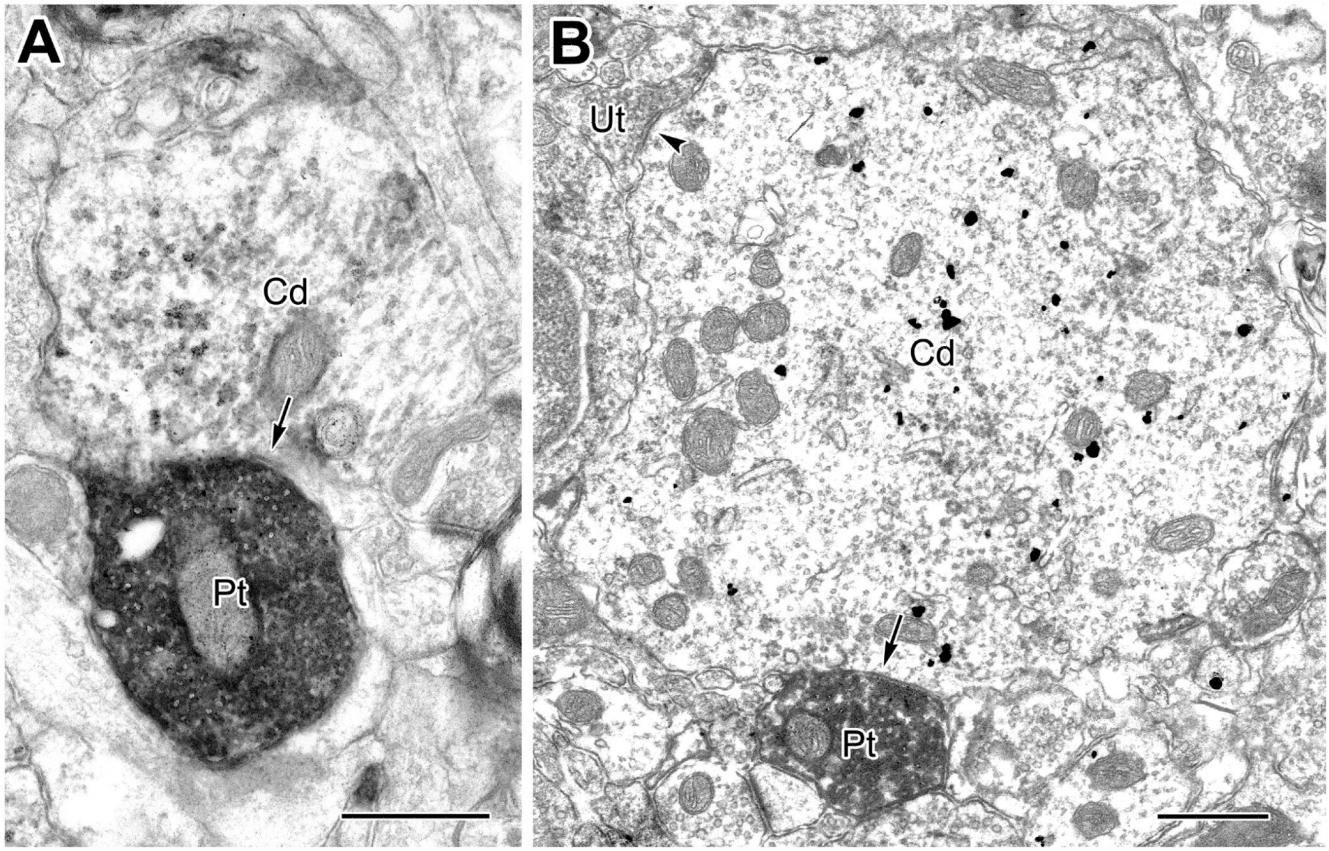

Figure 5.
Large caliber CaMK+ dendrites (Cd) receive synaptic input from PV+ terminals (Pt, arrows). **A:** A CaMK+ dendrite labeled by the V-VIP method receives synaptic input from a PV+ terminal. **B:** A CaMK+ proximal dendrite labeled by the IGS method receives input from a PV+ terminal. An unlabeled terminal, making symmetrical synaptic contact with the CaMK+ dendrite is also indicated (Ut, arrowhead). Scale bars = 0.5 μm.

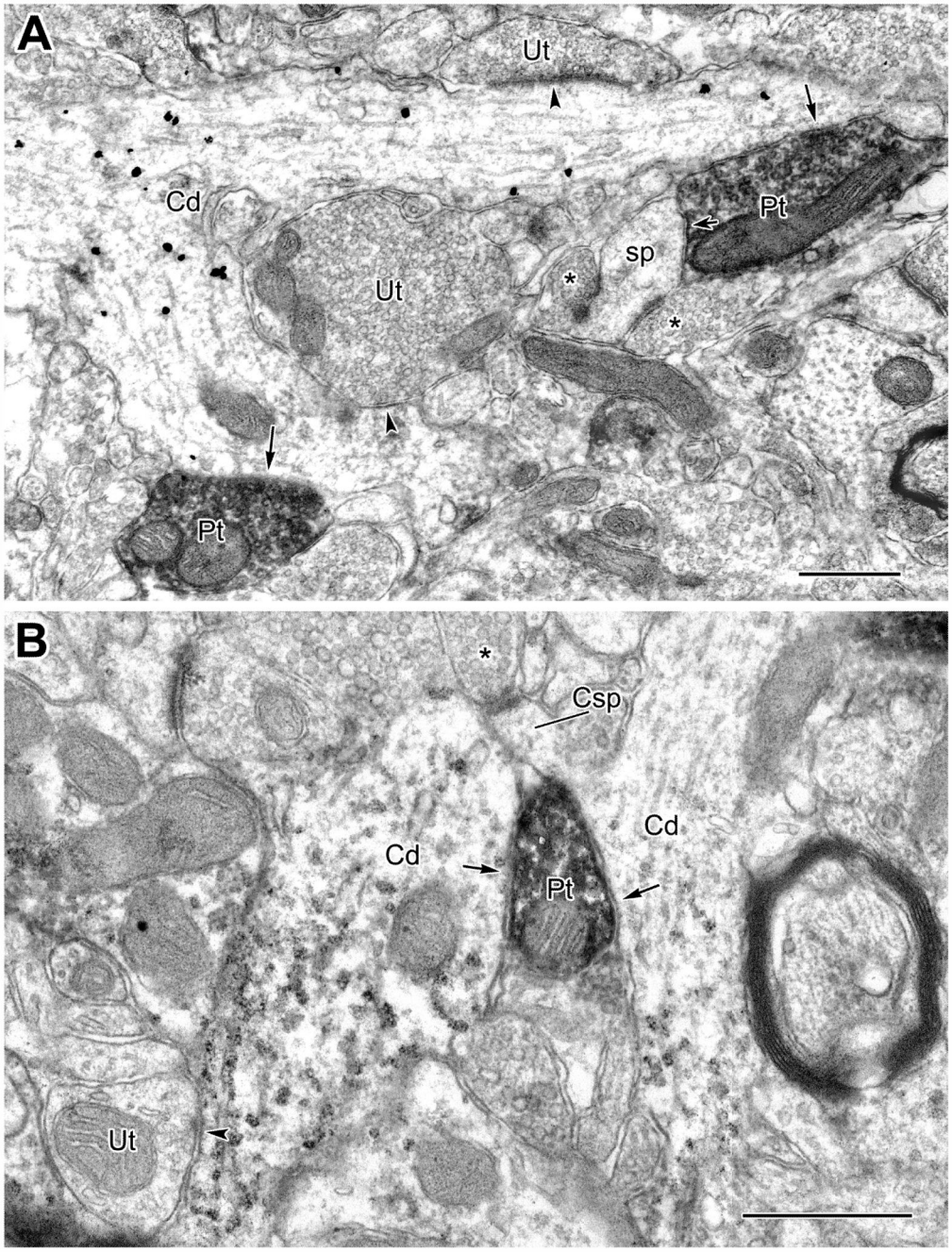

Figure 6.

Small caliber CaMK+ dendrites (Cd) receive synaptic input from PV+ terminals (Pt, arrows). **A:** A bifurcating CaMK+ dendrite, labeled by the IGS method, receives synaptic input from PV+ terminals on each of its branches. Each branch also receives symmetrical synaptic contact from unlabeled terminals (Ut, arrowheads). The PV+ terminal contacting the upper branch of the CaMK+ dendrite makes synaptic contact with a neighboring spine (sp, short arrow), which also receives additional synaptic input from two unlabeled terminals (asterisks). **B:** Two neighboring CaMK+ dendrites, labeled by the V-VIP method, receive synaptic input from the same PV+ terminal. The CaMK+ dendrite on the left also receives a symmetrical synaptic contact from an unlabeled terminal (Ut). The CaMK+ dendrite on the

right gives rise to a spine (Csp), which receives an apparent asymmetrical contact from an unlabeled terminal (asterisk). Scale bars = 0.5 μm.

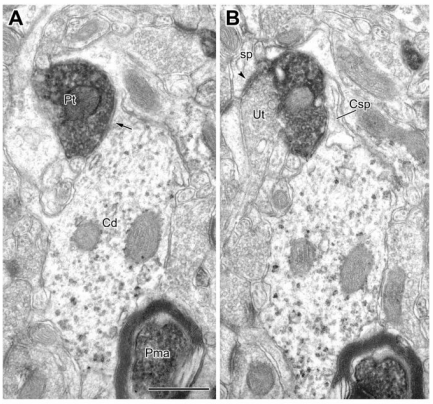

Figure 7.

A, B: Two serial sections of a CaMK+ dendrite (Cd) and emerging spine (Csp) receiving synaptic input from a PV+ terminal (Pt, arrow). The CaMK+ dendrite is labeled by the V-VIP method. A neighboring spine (sp) receiving an asymmetrical synaptic contact from an unlabeled terminal (Ut, arrowhead) and a PV+ myelinated axon profile (Pma) are also indicated. Scale bar = 0.5 μm.

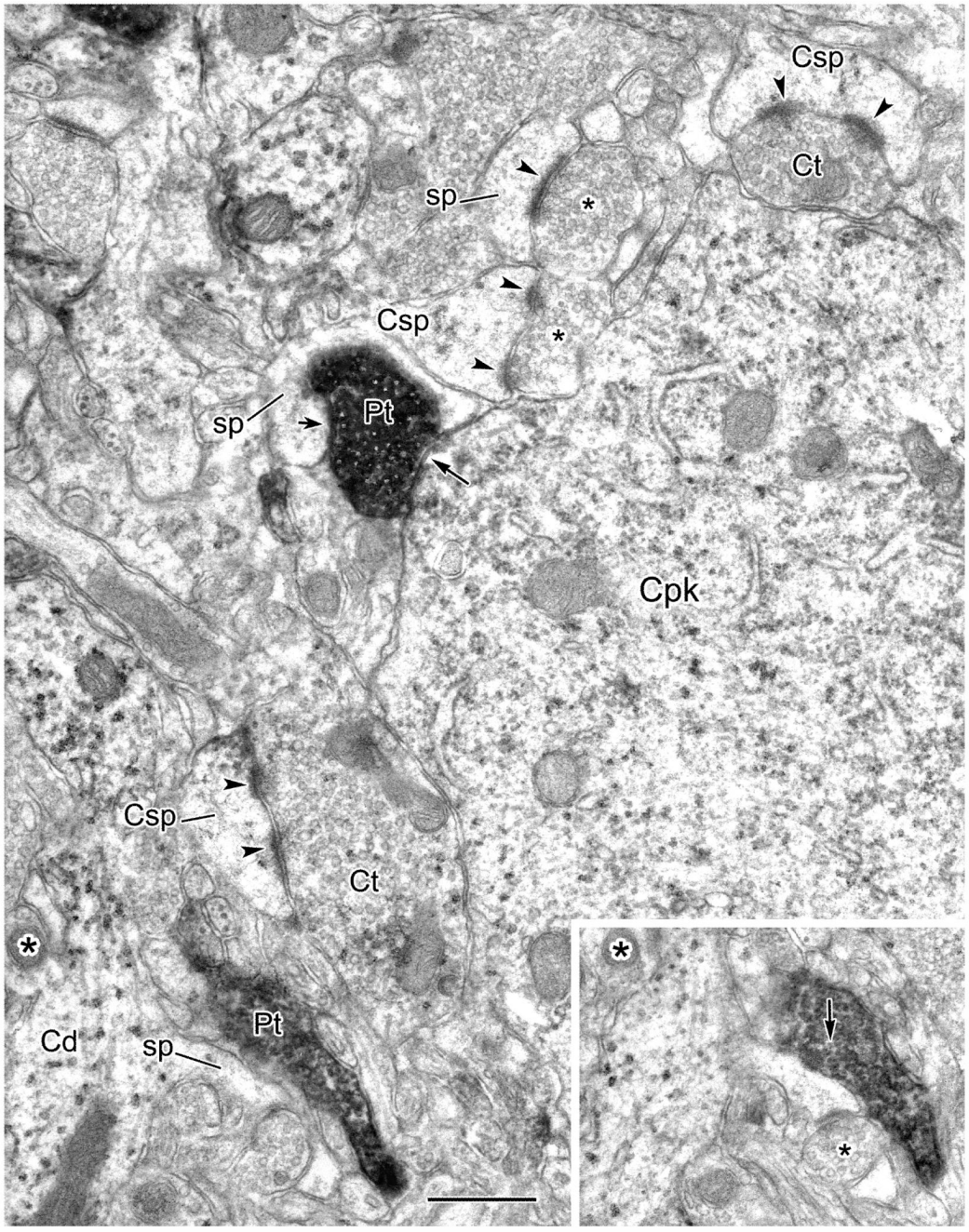

Figure 8.

Synaptic inputs to CaMK+ spines. Three CaMK+ spine heads (Csp), labeled with the V-VIP method, receive perforated asymmetrical synaptic input (pairs of arrowheads). Two of the terminals contacting the CaMK+ spines were also found, in serial sections, to be CaMK+ (Ct). Other terminals, with no apparent immunoreactivity (small asterisks), also make asymmetrical contact with spines. Two spines receive synaptic contacts from PV+ terminals (Pt). One of these spines (lower left) emerges from a CaMK+ dendrite (Cd), as shown in serial section in the inset. Large asterisks mark a common feature (a mitochondrion), for orientation. As seen in the inset, the emerging spine receives synaptic input from a PV+ terminal (arrow) as well as a small apparently unlabeled terminal (small asterisk). The other

PV+ terminal (left of center) makes synaptic contact with a spine (sp, short arrow) and a CaMK+ perikaryon (Cpk, arrow). The synaptic nature of the axosomatic contact was seen more clearly in adjacent serial sections. Scale bar = 0.5 μm.

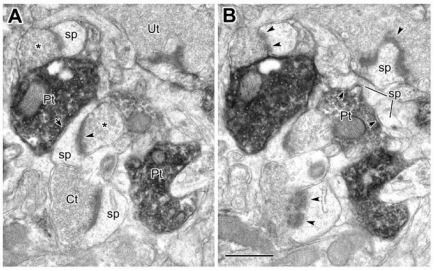

Figure 9.

Synaptic input to spines from PV+ terminals. **A, B:** Serial electron micrographs show synaptic inputs to spines (sp) from PV+ terminals (Pt, short arrows). **A:** One of the spines receiving input from a PV+ terminal (left center) also receives an asymmetrical synaptic contact from an unlabeled terminal (arrowhead, asterisk). Another spine (upper left corner) is shown to receive an asymmetrical contact only from an unlabeled terminal. A lightly labeled CaMK+ terminal (Ct) is shown in serial section (panel **B**) to make a perforated asymmetrical synaptic contact (two arrowheads) with a spine (sp). **B:** The PV+ terminal (Pt), central in the field, makes synaptic contact onto two emerging spines (sp, two short arrows), confirmed by additional serial sections. Scale bar = 0.5 μm.